

# Gamma Ray Irradiation Effects on Optical Elements of ITER Divertor Impurity Monitor<sup>\*)</sup>

Sin-iti KITAZAWA, Toshihiro OIKAWA, Hiroaki OGAWA, Tomohiro YOKOZUKA,  
Toshiyuki MARUYAMA and Suguru TANAKA

*Naka Fusion Institute, National Institutes for Quantum and Radiological Science and Technology (QST),  
Naka 311-0193, Japan*

(Received 10 January 2019 / Accepted 13 March 2019)

The ITER divertor impurity monitor (DIM) is a diagnostic system that directly observes 200 - 1000 nm light emissions from nuclear fusion plasma. Because the DIM observes a wide range of light from infrared to ultraviolet using a single optical system, high optical performance, such as spatial resolution and aberration, is required for the DIM optical elements. The DIM must be highly robust against external environmental factors, such as temperature, humidity, vibration, and magnetic field. Components having high radiation resistance must be used because of the high radiation environment in ITER. In this study, DIM optical elements installed in the interspaces and the port cells are investigated because gamma ray irradiation can impact their optical performance. The irradiation experiments were performed at QST's gamma-ray irradiation facilities in Takasaki. The attenuation of transmittance due to gamma irradiation were evaluated for silica, fluorite, and LiCaAlF<sub>6</sub> as the glass material in the spectrometers to be installed in the port cell. The influence of irradiation on silica polka dot beam splitters was found to be negligible; however, the transmittance of high OH concentration fibres for measuring UV light decreased significantly due to irradiation and will thus require countermeasures. The information necessary for proceeding with the ITER DIM design was obtained from these experimental results.

© 2019 The Japan Society of Plasma Science and Nuclear Fusion Research

Keywords: ITER, divertor impurity monitor (DIM), diagnostic system, nuclear fusion, gamma ray irradiation, LiCAF, LiCaAlF<sub>6</sub>, optical fibres, optical density

DOI: 10.1585/pfr.14.3405089

## 1. Introduction

ITER is an international project in which Japan, the USA, the EU, Russia, China, South Korea, and India are cooperating to build and operate a thermonuclear fusion experiment reactor [1]. ITER plasma diagnostic systems are used for plasma control, machine protection, and physics research. Approximately 50 diagnostic systems are procured by the participating parties. In the tokamak building, equipment for ITER diagnostics is installed in the vacuum vessel (VV), the interspaces (ISs) between the vacuum boundary and the biological shielding, and the port cells (PCs) on the outside of the biological shielding. Data is transferred to an acquisition system installed in the diagnostic building. The ITER divertor impurity monitor (DIM) system observes light from fusion plasma in the range from UV to near IR (200 - 1000 nm) in a single optical system. The DIM system has five optical elements in the Upper Port (UP) #01, Equatorial Port (EP) #01, and Lower Port (LP) #02 [2], where the optical systems in LP#02 consists of the one under the divertor dome and the ones at the gap between adjacent divertor cassettes. Light

observed is guided from the front-end optical system in the VV through ISs to PCs by using mirrors. The DIM system specifications are 50 mm for spatial resolution and 1 ms for time resolution, thus, very high optical performance is required, such as increasing the yield of light observed and suppressing aberration [3]. The DIM system observes 200 - 400 nm UV light, which is affected by the reduction of light transmittance due to the formation of a color center under a high gamma ray radiation environment. During the ITER engineering design activities (EDA) phase, radiation effects on the diagnostic instruments were studied [4]. However, as the design progressed, it became necessary to test and verify the latest equipment expected to be used in the actual equipment of ITER. The DIM equipment that was tested and verified in this study is from the present design and is summarized in Table 1, although the equipment may be updated as the design continues to progress.

For the DIM optical elements, front-end mirrors and reflectors are installed in the VV [5,6], steering mirrors and collection lenses are installed in the ISs, and steering mirrors, beam splitters, lenses and bandpass filters for spectrometers and optical fibres are installed in the PCs. In this study, the vacuum window is excluded as part of the VV. In the case of optical transmission by optical fibres from the light collecting system to the spectrometers, light longer

author's e-mail: kitazawa.siniti@qst.go.jp

<sup>\*)</sup> This article is based on the presentation at the 27th International Toki Conference (ITC27) & the 13th Asia Pacific Plasma Theory Conference (APPTC2018).

Table 1 DIM equipment for irradiation tests.

Optical element	
VV	Mirror: SS316L+Mo or Rh, SS316L+Al+ coat Retroreflector Mo or SS316L
IS	Mirror: (Base + Al + protective coat) Doublet lens: SiO <sub>2</sub> + CaF <sub>2</sub>
PC	Mirror: (Base + Al + protective coat, etc.) UV optical fibre, Vis/IR optical fibre Lens (SiO <sub>2</sub> , CaF <sub>2</sub> , LiCaAlF <sub>6</sub> , etc.) Half mirror (SiO <sub>2</sub> + Al + coat) Band pass Filter, Dichroic mirror
Electrical equipment	
VV	Limit switch for shutter, Thermocouple
IS	Piezoelectric actuator, Thermocouple
PC	Piezoelectric actuator, Thermocouple Light source for calibration CCD camera, E/O converter, power supply
Auxiliary equipment	
VV	Shutter System
PC	Epoxy filler in fibre bundles

Table 2 Estimated dose for DIM install space.

	Interspace IS	Port Cell PC
UP	1 - 8.4 MGy 0.2 - 1.8 kGy/h	1 - 5.6 kGy 0.2 - 1 Gy/h
EP	1 - 1.6 MGy 0.2 - 0.3 kGy/h	1 - 5.6 kGy 0.2 - 1 Gy/h
LP	1.3 - 5.5 MGy 0.3 - 1.2 kGy/h	0.1 - 180 kGy 0.02 - 40 Gy/h

than 400 nm has low attenuation and can be introduced to the spectrometers installed in the diagnostic building more than 100 m away from the PCs. Light in the 200 - 400 nm region, however, attenuates significantly. Hence, the spectrometers to measure UV light have to be installed near the collection optics in the PCs to shorten the optical fibres as much as possible. The UV signals are converted to electrical signals in the PCs.

Typical gamma ray doses in the ISs and the PCs at ports having no equipment or shielding where DIM equipment is installed are summarized in Table 2. These doses are calculated from the Radiation Map for the entire ITER tokamak. The minimum and maximum dose values in each space are also shown in Table 2. The doses were calculated by multiplying the dose rate by the total ITER operation time of 4,700 h. The doses are higher near the plasma because gamma rays are generated by radiation from the plasma or activation by neutrons. Here, the maximum value of the dose rate in the LP #02 PC is large because the piping for activated cooling water for divertors passes nearby. In this study, the maximum dose to be evaluated is taken as tolerances, 10 MGy in the ISs, and 200 kGy in the PCs.

In this study, we report the results of experiments on gamma ray irradiation effects on lens materials, polka-dot

beam splitters, and optical fibres.

## 2. Gamma Ray Irradiation Facility

Gamma ray irradiation experiments were performed at the gamma ray (<sup>60</sup>Co) irradiation facilities of QST's Takasaki Advanced Radiation Research Institute. Irradiations at dose rates of 0.4 to 10 kGy/h were done in the 2nd irradiation building capable of schedule irradiation, while those at lower dose rates were performed in the food irradiation building. The specimens were set at appropriate positions for their target dose rates based on a space dose rate map obtained by measuring using an ionization chamber and calibration using a polymethyl methacrylate (PMMA) dosimeter (Radix W) [7].

## 3. Gamma Irradiation on Lens Materials

The preliminary design of the DIM employs achromatic lenses in ISs and PCs and lens groups for spectrometers in PCs [3]. Silica (SiO<sub>2</sub>), fluorite (CaF<sub>2</sub>), and LiCAF (LiCaAlF<sub>6</sub>) were chosen as vitreous materials for the irradiation experiments. SiO<sub>2</sub> and CaF<sub>2</sub> are standard materials available on the market for optical elements whose types vary depending on their constituents and manufacturing processes. Materials having high radiation resistance have also been developed and the effects of gamma ray irradiation on them are well known. Therefore, the effects of gamma rays on materials from candidate manufacturers that are likely to be used in the actual equipment of the DIM system must be confirmed, which will contribute to the design of the shielding. LiCAF is a promising inorganic material for neutron scintillators and lasers and has undergone fundamental and application studies [8, 9]. LiCAF is also an advantageous material to use in the UV wavelength region due to its high Abbe number and thusly its high capability of chromatic aberration correction in the UV region. The effects of gamma ray irradiation on LiCAF must be investigated for LiCAF to be used in ITER radiation environments. The glass material specimens were procured from Bunkoukeiki Co., Ltd. [10], a candidate manufacturer for the spectrometers. The dimensions of specimens are 10 × 7 × 4.1 mm for SiO<sub>2</sub>, 10 × 7 × 4.0 mm for CaF<sub>2</sub>, and 10 × 7 × 5.2 mm for LiCaAlF<sub>6</sub>.

### 3.1 Gamma irradiation effects on silica

The transmittance spectra of SiO<sub>2</sub> specimens were measured using a spectrophotometer (JASCO V-750) at each step of gamma ray irradiation, as shown in Fig. 1. The small peak at 400 nm was caused by a filter in the spectrometer, the step at 340 nm was caused by switching the light source. The gamma ray induced color centers of SiO<sub>2</sub> are dominated by non-bridging oxygen hole centers NBOHC (≡Si-O ·) with a peak at 260 nm and E'-center (≡Si ·) with a peak at 215 nm. In the region above 400 nm where these effects are absent, the decrease in transmit-

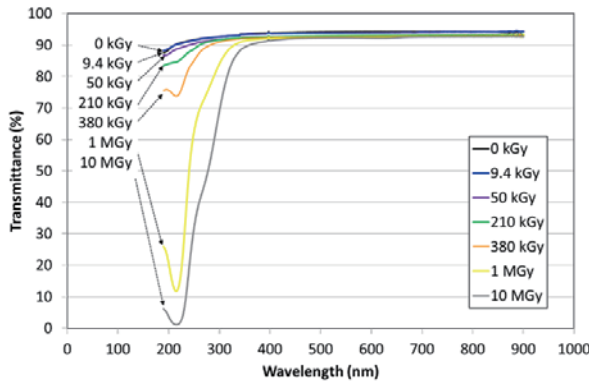


Fig. 1 Transmittance spectra of silica glass specimen (4.1 mm thickness) after  $^{60}\text{Co}$  gamma ray irradiation.

tance at 10 MGy irradiation is about 2%. However, the transmittance decreases with the doses in the region below 300 nm due to the color centers and becomes extremely low near 215 nm at 10 MGy.

Irradiation-induced degradation of transmittance has to be minimized as much as reasonably achievable. In the ISs, when assuming the transmittance of a  $\text{SiO}_2$  lens having a thickness of 4 mm after 10 MGy of irradiation has to be kept above 80% over the entire wavelength region of DIM measurements, the 10 MGy dose must be reduced to about 250 kGy by shielding. This reduction is equivalent to 6cm-thick tungsten, 10-cm thick lead, or 22-cm thick stainless steel for shielding  $^{16}\text{N}$  gamma rays. However, shielding of the optical elements may not be easy because gamma rays can also reach along the optical path. In the PCs, the transmittance needs to be as high as possible because many silica materials are used for lenses, band-pass filters, and other elements in the spectrometers. In the region of 200 - 300 nm, the transmittance drop of an optical fibre is relatively large (5 - 10%) even without the effects of irradiation and the gamma irradiation-induced attenuation of transmittance (about 10%) was observed for a 4.1-mm thick silica specimen at a dose of 200 kGy. Therefore, the design of PC optics must be improved by taking into account a simple optical configuration, choice of glass materials, layout of optical elements having different radiation resistance, and reasonable and realistic shielding that fits in the narrow assigned space in the PCs.

### 3.2 Gamma irradiation effects on fluorite

The transmittance spectra of  $\text{CaF}_2$  specimens after gamma ray irradiation are shown in Fig. 2. The measurements were performed in the same manner as with  $\text{SiO}_2$ . Neither major color center nor irradiation-induced attenuation of transmittance were observed. No special consideration needs to be taken for  $\text{CaF}_2$  as regards the design of the DIM optical system because  $\text{CaF}_2$  is used together with  $\text{SiO}_2$  to correct the chromatic aberration of  $\text{SiO}_2$ , thus, the radiation shielding for  $\text{SiO}_2$  is sufficient for  $\text{CaF}_2$ .

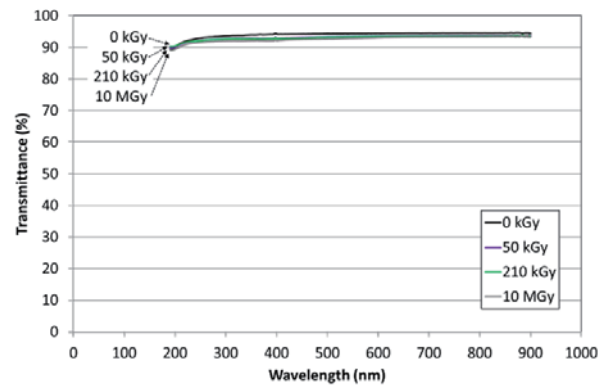


Fig. 2 Transmittance spectra of  $\text{CaF}_2$  specimen (4.0 mm thickness) after  $^{60}\text{Co}$  gamma ray irradiation.

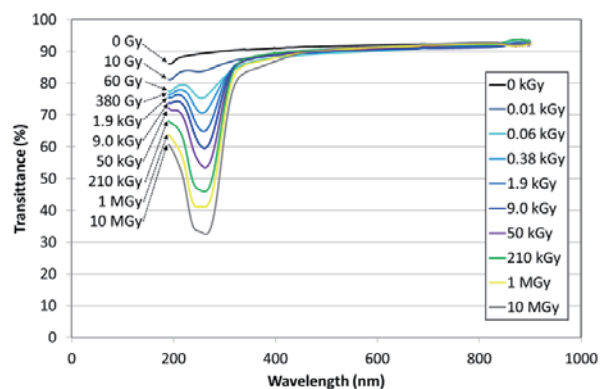


Fig. 3 Transmittance spectra of LiCAF glass specimen (5.2 mm thickness) after  $^{60}\text{Co}$  gamma ray irradiation. Absorption due to the F center at 262 nm and transition at 245 nm are apparent.

### 3.3 Gamma irradiation effects on LiCAF

The transmittance spectra of  $\text{LiCaAlF}_6$  specimens after gamma ray irradiation are shown in Fig. 3. Compared with  $\text{SiO}_2$ , the transmittance decreases in the wavelength region lower than 400 nm even at low doses, but saturation occurs at doses of several MGy. It would be difficult to use  $\text{LiCaAlF}_6$  in an optical system in a gamma ray environment because a 5% reduction near 250 nm was observed at an irradiation of only 10 Gy. The advantage of LiCAF glass is its correction of chromatic aberration in the UV region. However, its superiority would be lost due to its low transmittance in the UV region in a radiation environment.  $\text{LiCaAlF}_6$  glass has a color center of F-center at 262 nm [8], which can be observed in terms of its optical density (absorbance). The optical density per unit length  $\text{OD}(\lambda) / d$  [ $\text{cm}^{-1}$ ] is calculated from the formula (1), where transmittance is  $T(\lambda)$ , reflectance is  $R(\lambda)$ , and sample thickness is  $d$  (cm). The reflectance measured is taken into consideration.

$$\text{OD}(\lambda)/d = -\log_{10} [T(\lambda)/(1 - R(\lambda))] / d. \quad (1)$$

The optical density of a LiCAF specimen at the F-

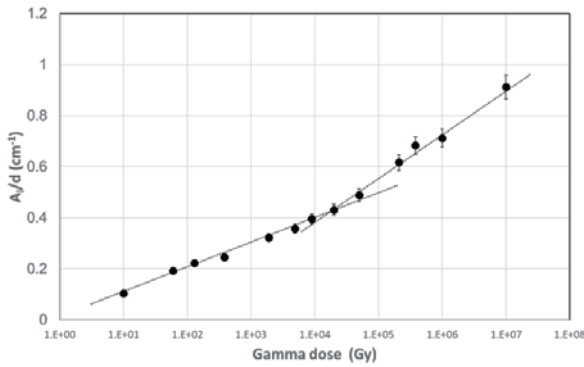


Fig. 4 Optical density of LiCAF glass specimen at 262 nm after  $^{60}\text{Co}$  gamma ray irradiation. Below 10 kGy, the contribution from the  $F$  center at 262 nm is dominant, and the influence by transition of electron trapped at  $F$  center is apparent above 20 kGy.

center (262 nm) is shown in Fig. 4. The error bars on the optical density were added as measurement error. The plot increases with the same slope up until about 10 kGy, after which the slope becomes steeper. This difference in slope is owing to the dominant effect of  $F$ -center when the number of color centers is small, however, the transition of a single electron trapped in the  $F$ -center  $F^0 \rightarrow F^+$  (245 nm) increases with the number of color centers. Here,  $F^+$ ,  $F^0$ , and  $F^-$  mean the states that the  $F$  center can trap 0, 1, and 2 electrons, respectively. At low doses, the contributions from the formation of the  $F$ -center (absorption at 262 nm) is dominant, and over 10 kGy, the contributions by the generated  $F$ -center are apparent.

#### 4. Gamma Irradiation on Beam Splitters

The DIM has three kinds of spectrometers, a filter spectrometer for observation of a fixed wavelength at a high time resolution, a survey spectrometer that measures over a wide wavelength region simultaneously, and a high dispersion spectrometer at a high wavelength resolution [11]. Therefore, it is necessary to distribute the observed light to spectrometers without wavelength dependence in the measurement range (200 - 1000 nm) by using beam splitters. Several methods for splitting light have been studied, such as branching using optical fibres [4]. A simple optical system to divide incident light is necessary because optical components are installed in the narrow assigned space in the PCs. A polka-dot mirror, which is formed by vapor depositing small, circular mirrors on a glass form is considered to be a promising candidate. The effects of gamma ray irradiation on transmittance, reflectance, and morphology were investigated.

The specimen is a Shimadzu T50-20S fused silica base Al dotted mirror with  $\text{MgF}_2$  protection coating, which is a so-called half mirror having approximately 50% reflection. Its dimensions are  $50.8 \times 50.8 \times 1.5$  mm and its dot

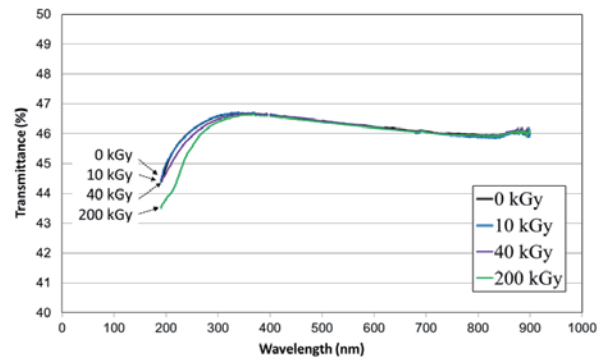


Fig. 5 Transmittance spectra of polka-dot half mirror after  $^{60}\text{Co}$  gamma ray irradiation.

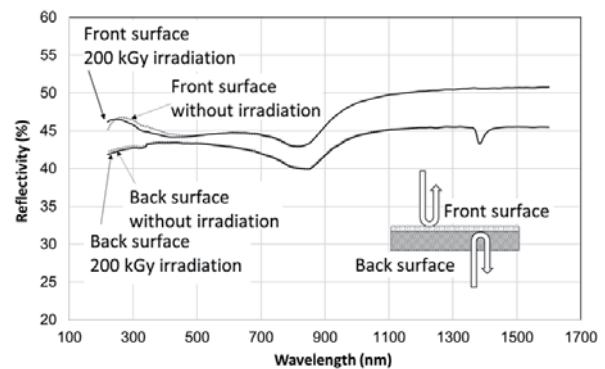


Fig. 6 Reflectance spectra of polka-dot half mirror after  $^{60}\text{Co}$  gamma ray irradiation.

pitch is about 0.3 mm [12].

The transmittance spectra of polka-dot half mirrors after gamma irradiation are shown in Fig. 5. A small peak at 400 nm that was caused by an internal filter of the spectrophotometer was removed to avoid any misinterpretations. The measurement conditions were the same as those of the measurements of the lens materials. Since the polka-dot mirror is designed as a 50% reflecting half mirror, it shows characteristics similar to those of  $\text{SiO}_2$  in Fig. 1 having a maximum transmittance of 50%.

The reflectance spectra of polka-dot half mirrors are shown in Fig. 6. The reflections of the front coated surface and the back substrate surface were measured using a JASCO V-780 spectrophotometer with a SLM-907 specular reflectance accessory having a  $5^\circ$  incident angle. The multi surface reflections were not excluded. For back reflection, an absorption peak of silica ( $\equiv\text{Si}-\text{OH}$ ) was observed near 1390 nm. No significant effects from irradiation were observed in the range up to 200 kGy on both the surface reflection and the back reflection.

SEM observations were carried out to investigate the morphology of the polka-dot half mirrors after irradiation. SEM images before and after 200 kGy of irradiation are shown in Figs. 7A and 7B, respectively. The accelerating voltage of the electron beam was 2 kV. The circles are



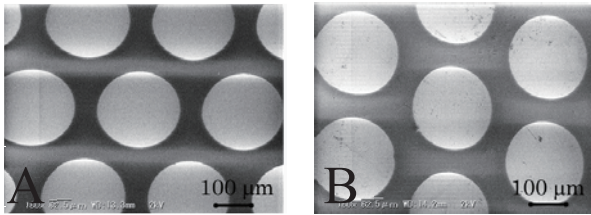


Fig. 7 SEM images of polka-dot half mirror. A) Before irradiation, B) 200 kGy irradiation.

the Al-deposited surface on the fused silica substrate. The electric conductance of the protective coat of  $\text{MgF}_2$  is low so that the electron charge-up produces some noise. Any visible damage due to gamma ray irradiation is not observed along the edges of the aluminum circles.

From these results, it was found that the impact on optical performance by gamma ray irradiation of approximately 200 kGy would be negligible if a polka-dot beam splitter is used in the PCs.

## 5. Gamma Irradiation on Optical Fibres

Optical fibres are widely used in various gamma ray environments. Research was also carried out in the engineering design phase of ITER [13, 14]. In most of this research, the wavelength region evaluated was mostly longer than 400 nm, while the DIM system measures 200–1000 nm. Hence, it is necessary to evaluate the optical characteristics after irradiation in the UV range of 200–400 nm. The DIM system employs optical fibres to transmit collected light by a telescope to the UV spectrometers in the PCs and to the Vis/IR spectrometers in an external building. The length of UV optical fibres in the PCs are less than 5 m and the length of Vis/IR is about 10 m in the PCs and over 100 m in non-radiation areas [11]. We conducted preliminary experiments on the effects of gamma ray irradiation on high OH concentration optical fibres and low OH concentration fibres, which are used for measurements in the UV region and the Vis/IR region, respectively.

Optical systems were set up as shown in Figs. 8(a) and 8(b) to measure the change in transmittance due to gamma ray irradiation of optical fibres. In both systems, the gamma-irradiated optical fibres were connected to a light source and a polychromator via connection fibres to adjust the amount of light and convert FC connectors to SMA connectors. The light source for UV was a  $\text{D}_2$  lamp (Hamamatsu L 10290) and the light source for Vis/IR was an integrating sphere light source (HELIOS). Avantes AvaSpec-2048L polychromators were used to measure UV (200–450 nm) and Vis/IR (350–1100 nm) using different gratings. The optical fibre specimens were Fujikura FFC-2P-2M-S 200/220 high OH type for UV and FFC-2P-2M-S, and 200/220B low OH type for Vis/IR. The core diameters were 200  $\mu\text{m}$ , the lengths were 2 m, and FC connec-

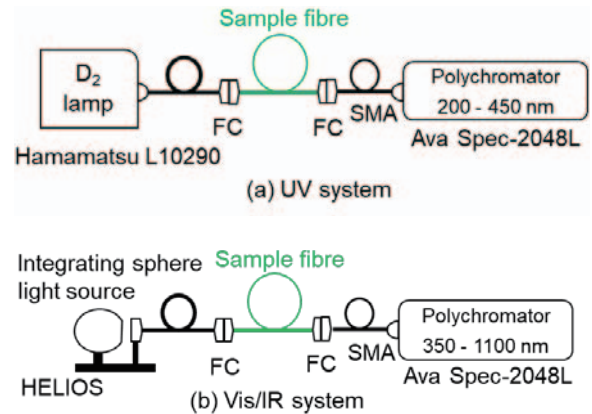


Fig. 8 Optical system used for measuring transmittance of optical fibres. (a) UV measurement (b) Vis/IR measurement.

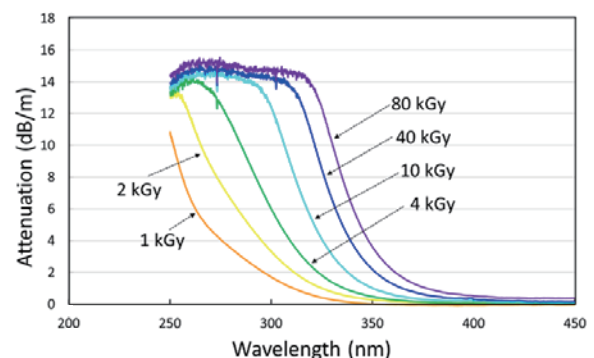


Fig. 9 Radiation-induced attenuation spectra of high OH fibres for UV in UV region by  $^{60}\text{Co}$  gamma ray irradiation.

tors were attached at both ends [15]. The technical specification shows the spectral attenuation are 0.1 dB/m in the region longer than 400 nm, and spectral attenuation drops sharply as the wavelength becomes shorter.

The observed radiation-induced attenuation (RIA) spectra in the UV region of the high OH fibre is shown in Fig. 9. The horizontal axis is wavelength, and the vertical axis indicates the ratio of the transmittance of the irradiated fibres to that of unirradiated fibres. Because the signal of the transmitted light in the region under 250 nm was quite small, that area was not included in the figure. The observed decrease in the region under 300 nm is significant even at 1 kGy of irradiation. In particular, in the region around 250 nm, the transmittance is very weak. As the irradiation increases, the transmittance on the shorter wavelength becomes lower. Consequently, the attenuation of the light transmittance in the UV range due to gamma ray irradiation is very large and some remedial measures should be considered.

The results of RIA spectra in the Vis/IR region of the low OH fibres are similar to the results from former experiments [6]. The decrease of transmittance of the low OH fibre in the Vis/IR region is negligible for its use in PCs with reasonable radiation shielding. The next step for op-

tical fibres is to conduct gamma ray irradiation on the fibre bundle assemblies.

## 6. Summary

Gamma ray irradiation tests for DIM optical elements that are installed in the ITER radiation environment were carried out for the final design. For the lens materials, we found that the use of silica and LiCAF requires more shielding for 10 MGy irradiation in the ISs. For LiCAF, it was observed that the absorption due to the generated F-centers becomes prominent over 1 MGy. For polka-dot beam splitters, it was found that the effects of gamma ray irradiation on the reflectance and transmittance was negligible for its use in the PCs. For optical fibres, it was found that the attenuation of the transmittance of the high OH fibre for UV measurement is significant and hence it is necessary to make design improvements in terms of transmission of light in the PCs, such as enhanced radiation resistance of a fibre combined with shielding or an alternative optical configuration without fibres. Further gamma ray irradiation tests on the ITER DIM system design are necessary to improve and secure the performance of each optical/mechanical/structural/electrical component.

## Acknowledgments

We appreciate the members of the QST Plasma Di-

agnostic Group for their valuable advice in carrying out this study. We would like to thank Naotsugu Nagasawa and Hajime Seito for the implementation of the gamma ray irradiation experiments. We would like to thank Shunya Yamamoto, Hiroshi Koshikawa, and Masaki Sugimoto for their cooperation during the observation including Nathaniel Duncan for his help with making this manuscript.

- [1] D.J. Campbell *et al.*, “Innovations in Technology and Science R&D for ITER”, *J. Fusion Energy* **38**, 11 (2019).
- [2] H. Ogawa *et al.*, *Fusion Eng. Des.* **83**, 1405 (2008).
- [3] S. Kitazawa *et al.*, *Fusion Eng. Des.* **101**, 209 (2015).
- [4] T. Nishitani *et al.*, “Irradiation Effects on Plasma Diagnostic Components (II)”, *JAERI-Research 2002-007* (2002).
- [5] A. Iwamae *et al.*, *Rev. Sci. Instrum.* **82**, 033502 (2011).
- [6] T. Takemoto *et al.*, *Optik* **127**, 2950 (2016).
- [7] M. Takehisa *et al.*, *Radiat. Phys. Chem.* **76**, 1619 (2007).
- [8] H. Sato *et al.*, *J. Appl. Phys.* **91**, 5666 (2002).
- [9] M.-H. Du and D.J. Singh, *J. Appl. Phys.* **112**, 123516 (2012).
- [10] <http://www.bunkoukeiki.co.jp/>
- [11] S. Kitazawa *et al.*, *Fusion Eng. Des.* **112**, 74 (2016).
- [12] <https://www.shimadzu.com/>
- [13] T. Kakuta *et al.*, *Fusion Eng. Des.* **41**, 201 (1998).
- [14] T. Shikama *et al.*, *Nucl. Fusion* **43**, 517 (2003).
- [15] <http://www.fujikura.co.jp/>